Bone 124 (2019) 53–61

Contents lists available at ScienceDirect

Bone

journal homepage: www.elsevier.com/locate/bone

Full Length Article

IL-6 and sIL-6R induces STAT3-dependent differentiation of human VSMCs into osteoblast-like cells through JMJD2B-mediated histone demethylation of *RUNX2*

Akira Kurozumi, Kazuhisa Nakano, Kaoru Yamagata, Yosuke Okada, Shingo Nakayamada, Yoshiya Tanaka*

The First Department of Internal Medicine, School of Medicine, University of Occupational and Environmental Health, Japan, Kitakyushu 807-8555, Japan

ARTICLE INFO

Keywords:
Cytokines
Transcription factors
Osteoblasts
Disorders of calcium/phosphate
Epigenetics

ABSTRACT

Inflammation and vascular calcification are independent risk factors of cardiovascular events. Vascular smooth muscle cells (VSMCs) exhibit osteoblast-like characteristics in response to various stimuli such as oxidized cholesterol and inflammation. However the precise mechanism of transcriptional regulation of VSMCs by inflammatory stimuli remains unclear. We investigated the process and mechanisms of inflammatory cytokine-induced transformation of human VSMCs (hVSMCs) into osteoblast-like cells, with a special focus on epigenetic changes. Our results demonstrated: (1) interleukin-6 (IL-6)/soluble interleukin-6 receptor (sIL-6R) induced transformation of hVSMCs into an osteoblast phenotype, with subsequent vascular calcification, based on the results of Alizarin Red S staining and O-Cresolphthalein complexone method; (2) IL-6/sIL-6R accelerated the expression of runt-related transcription factor 2 (RUNX2) based on the results of quantitative real-time polymerase chain reaction; (3) Knockdown of signal transducer and activator of transcription (STAT) 3 reduced IL-6/sIL-6R-induced RUNX2 mRNA expression and osteoblast transdifferentiation of hVSMCs; (4) Chromatin immunoprecipitation (ChIP) coupled with PCR (ChIP-PCR) identified a STAT-binding site in *RUNX2* promoter region containing trimethylated histone 3 lysine 9 (H3K9me3), a transcriptional repressor, and H3K4me3, a transcriptional enhancer. Stimulation with IL-6/sIL-6R suppressed H3K9me3 but not H3K4me3 through the recruitment of jumonji domain-containing protein (JMJD) 2B, a histone lysine demethylase, at the STAT-binding site in *RUNX2* promoter region; (5) IL-6/sIL-6R-induced *RUNX2* gene expression was inhibited in hVSMCs pretreated with JIB04, JMJD2 inhibitor, and the inhibitory effect was JIB04 dose-dependent. Our results indicate that the IL-6/STAT3/JMJD2B pathway regulates hVSMCs differentiation into osteoblast-like cells, which suggest its pathogenic role in vascular calcification associated with chronic inflammation.

1. Introduction

Mönckeberg's medial calcification, a common complication in patients with chronic kidney disease (CKD) and diabetes mellitus, is a known risk factor for macroangiopathy and associated with poor prognosis [1,2]. Vascular smooth muscle cells (VSMCs) exhibit osteoblast-like characteristics in response to various stimuli, such as oxidized cholesterol and inflammation [3]. Under such conditions, cultured VSMCs do not only express master transcription factors for osteoblast differentiation (e.g., *runt-related transcription factor 2 (RUNX2)* and *muscle segment homeobox 2 (MSX2)*), but also markers of osteoblast differentiation [e.g., *alkaline phosphatase (ALP)*, *osteopontin (OPN)*, and *osteocalcin (OC)*], thereby inducing vascular calcification [4]. In patients with CKD and those on chronic dialysis, hyperphosphatemia is one of the most important etiological factors of vascular calcification [5], whereas high levels of oxidative stress [6], serum C-reactive protein (CRP), inflammatory cytokines, and others are known as risk factors for cardiovascular diseases [7].

Serum levels of interleukin-6 (IL-6), a typical pro-inflammatory cytokine, increase with deterioration of renal dysfunction, while a high cardiovascular mortality rate has been reported in patients with high serum IL-6 [8]. Also Caselli et al. reported that serum IL-6 elevation can be a risk factor for mortality due to coronary artery disease [9] and IL-6 is an independent predictor of mortality in patients starting dialysis

* Corresponding author at: The First Department of Internal Medicine, School of Medicine, University of Occupational and Environmental Health, Japan, 1-1 Iseigaoka, Yahatanishi-ku, Kitakyushu 807-8555, Japan.
E-mail address: tanaka@med.uoeh-u.ac.jp (Y. Tanaka).

https://doi.org/10.1016/j.bone.2019.04.006
Received 19 December 2018; Received in revised form 30 March 2019; Accepted 11 April 2019
Available online 11 April 2019
8756-3282/

treatment [10]. Hénaut L et al. reported that IL-6 is a well-known inducer of VSMC osteogenic transition and mineralization [11], and is also a significantly better predictor of mortality risk than other inflammation markers such as C-reactive protein, albumin or TNF-α in patients with chronic kidney disease. In vitro studies have demonstrated that IL-6 enhances calcification related gene expression and calcification in VSMCs [12,13]. However, the precise mechanisms of transcriptional regulation of VSMCs by IL-6 remain unclear.

Epigenetic modifications are changes in gene expression that are not caused by modification in deoxyribonucleic acid (DNA) sequence. Epigenetic alterations, such as DNA methylation and histone modification, are essential in the regulation of differentiation of tissue stem cells in adults, in addition to embryonic development and cell differentiation [14,15]. These mechanisms are also thought to be associated with transformation of VSMCs into osteoblast-like cells. However, there are still many unknown aspects of the mechanisms underlying transformation of VSMCs into osteoblast-like cells. In particular, the molecular mechanisms involved in this process under inflammatory conditions remain elusive. Elucidation of epigenetic modifications that induce VSMCs transformation can potentially contribute to the development of cell-specific and effective treatment strategies.

The present study was designed to define the process and determine the mechanism by which inflammatory cytokines mediate the transformation of human VSMCs (hVSMCs) into osteoblast-like cells, with a particular focus on epigenetic changes.

2. Materials and methods

2.1. Cells

hVSMCs were purchased from Kurabo (Osaka, Japan) and cultured in Dulbecco's modified Eagle's medium (DMEM) (low glucose: 5.5 mM) containing 10% heated-inactivated fetal bovine serum (FBS) and supplemented with sodium pyruvate (1 mmol/l), penicillin (100 U/ml) and streptomycin (100 U/ml) at 37 °C in a 5% CO_2 atmosphere. The medium was replaced with a fresh medium every 3 days. The hVSMCs from passages 4–7 were used in this study. For this purpose, 2.5×10^4 hVSMCs were seeded onto 24-well plates (Corning, Corning, NY) and cultured in osteoblast-induced medium (OIM) (50 μM ascorbic acid, 10 mM β-glycerophosphoric acid and 0.1 μM dexamethasone). All media were obtained from Lonza. The ethics approval for the experiments using hVSMCs was granted by the Ethics Committee of the University of Occupational and Environmental Health, Japan.

hVSMCs-conditioned medium assay - In this assay, hVSMCs (2.5×10^4 cells) were seeded onto 24-well plates and cultured in OIM at 37 °C under 5% CO_2 atmosphere. Recombinant human TNF-α (R&D Systems, Minneapolis, MN), human IL-1β (RELIATech, Wolfenbuttel, Germany) or IL-6 (Miltenyi Biotec, Bergisch Gladbach, Germany) with human sIL-6R (R&D Systems) were added to OIM. The medium was replaced every 3 days throughout the experiments. JIB04, a pan-jumonji histone demethylase inhibitor, was purchased from R&D Systems.

2.2. Quantitative RT-PCR

Total mRNA was collected with the RNeasy Mini Kit (Qiagen, Hilden, Germany) and cDNA was obtained by reverse transcription according to the instructions provided by the manufacturer. RT-PCR was performed using primers specific for *RUNX2* (Hs01047978_m1), *MSX2* (Hs00751239_s1), *bone morphogenetic protein-2 (BMP2)* (Hs00154192_m1), *Pit-1/SLC20A1* (Hs00965587_m1), *Pit-2/SLC20A2* (Hs00198840_m1), *ALP (ALPL)* (Hs01029144_m1), *OPN (SPP1)* (Hs00960942_m1), *osterix (OSX) (SP7)* (Hs01866874_s1), *α-smooth muscle actin (α-SMA) (ACTA2)* (Hs00426835_g1), *smooth muscle myosin heavy chain (SM-MHC) (MYH11)* (Hs00224610_m1) (Applied Biosystems, Foster City, CA). *RUNX2, MSX2, BMP2, Pit-1/SLC20A1, Pit-2/SLC20A2, ALP, OPN, OSX, α-SMA* and *SM-MHC* were normalized to the levels of GAPDH (Taqman probe Hs99999905_m1) as the endogenous control and calculated using the $\Delta\Delta C_T$ method. The Jumonji domain-containing proteins (JMJD) 2 primer designs are listed in Supplementary Table (Eurofin Genomics: Louisville, KY).

2.3. Mineralization assay

Cell mineralization was evaluated by Alizarin Red S (ARS) staining (Sigma-Aldrich, St Louis, MO). Briefly, cells were cultured under the indicated conditions in a 24-well plate and fixed with 10% formaldehyde for 15 min then rinsed with deionized water before adding 350 μl of 1% ARS solution (pH 4.1) per well. After 15-min incubation at room temperature, the cells were washed with deionized water.

2.4. Quantification of calcification deposit

The calcium content of HCl supernatants was determined colorimetrically using the O-Cresolphthalein complexone (OCPC) method (Metallogenics). The Calcium Assay Kit is a direct colorimetric assay based on the OCPC method and does not require deproteinization of the sample. Determination of calcium contents is based on the reaction of calcium with OCPC in alkaline solution, which yields a violet colored complex. The intensity of the violet color is proportional to the calcium concentration in the sample. Absorbance of the Ca^{2+}–O-Cresolphtalein complex is measured at 570 nm, with wavelength range of sensitivity of 560–590 nm.

2.5. Western blot analysis

Cells were washed twice with cold phosphate-buffered saline (PBS) and dissolved with lysis buffer containing 50 mM Tris (pH 8.0), 150 mM NaCl, protease inhibitor and 10% NP-40. Equal amounts of protein (20 μg) were electrophoresed by SDS-PAGE, transferred onto nitrocellulose membranes and blotted with antibodies against STAT1, STAT3, p-STAT1, p-STAT3 (Cell Signaling Technology, Beverly, MA) or β–actin (Sigma-Aldrich), followed by incubation with secondary antibodies (GE Healthcare, Chalfont St Giles, UK).

2.6. Small interfering-RNA

siRNAs were purchased from Invitrogen (Carlsbad, CA) and their primer designs are shown in Supplementary Table. The negative control siRNA had low GC: 12935–200 and high GC: 12935–400. Transfection was performed using lipofectamine RNAiMAX (Invitrogen). In brief, hVSMCs (2.5×10^4 cells) were plated onto a 24-well plastic plate in 500 μl of antibiotic-free DMEM one day before transfection. On the next day, transfection reagents containing 7.5 pmol siRNA, 0.75 μl lipofectamine RNAiMAX in a final volume of 50 μl with FBS-free DMEM were added to each well and incubated with IL-6 (100 ng/ml) and sIL-6R (100 ng/ml) for 48 or 72 h.

2.7. ChIP assay

The ChIP analysis was carried out using EZ-ChIP (Millipore, Billercia, MA). Rabbit and mouse IgG were used as the negative control. Briefly, hVSMCs were cross-linked in 1% formaldehyde for 10 min and lysed in SDS lysis buffer and then sonicated to shear DNA. After dilution of the lysates with ChIP dilution buffer, they were immunoprecipitated with rabbit or mouse IgG, anti-acetylated histone 3 lysine 9 (H3K9ac) antibody, anti-trimethylated histone 3 lysine 4 (H3K4me3) antibody, anti-trimethylated histone 3 lysine 9 (H3K9me3) antibody, anti- trimethylated histone 3 lysine 27 (H3K27me3) antibody and anti-trimethylated histone 3 lysine 36 (H3K36me3) antibody (Monoclonal Antibody Institute, Sapporo, Japan), anti-acetylated histone 3 lysine 14 (H3K14ac) antibody (Cell Signaling, Danvers, MA), anti-JMJD2A

antibody, anti-JMJD2B antibody and anti-JMJD2C antibody (Bethyl laboratories, Inc.) overnight at 4 °C. The antibody-chromatin complexes were precipitated with ChIP blocked protein G agarose for 1 h at 4 °C and then washed and eluted. After reverse crosslink of protein-DNA complexes, DNA was purified using spin columns and analyzed by real-time PCR. The *RUNX2* primer design is described in Supplementary Table (Eurofin Genomics).

2.8. Immunocytochemistry

First, hVSMCs were fixed with 3% paraformaldehyde for 20 min and incubated with 0.5% triton X-100 for 10 min at room temperature. Then, they were incubated with antibodies against JMJD2A, JMJD2B and JMJD2C (Bethyl laboratories, Inc.) for 2 h, followed by fluorescein isothiocyanate (FITC)-conjugated anti-rabbit IgG (Sigma) at saturating concentrations in a medium consisting of HBSS (Nissui, Tokyo), 0.5% human serum albumin (Mitsubishi Pharma, Osaka, Japan), and 0.2% NaN_3 (Sigma) for 2 h at room temperature.

2.9. Statistical analysis

Data are expressed as mean ± SD. Differences between two groups were tested for statistical significance using the two samples *t*-test. Differences between three or more groups were tested for statistical significance using ANOVA test. In all analyses, a *P*-value < 0.05 was considered significant.

3. Results

IL-6/sIL-6R accelerated differentiation of hVSMCs into osteoblast-like cells.

First, we investigated the effects of inflammatory cytokines on osteoblast-like differentiation of hVSMCs. For this purpose, hVSMCs were cultured in the presence of TNF-α, IL-1β or IL-6/soluble IL-6 receptor (sIL-6R) (0.01–100 ng/ml). On culture day 21, calcification was assessed by Alizarin Red S (ARS) staining (Fig. 1A). In the in vitro osteoblast differentiation assay, matrix maturation and mineralization are usually enhanced by growing the cells to complete confluence and by adding specific osteogenic factors [16]. Therefore, differentiation of osteoblasts in vitro usually takes about 14 to 21 days. The selection of day 21 for ARS staining was based on a series of preliminary experiments that showed complete hVSMCs differentiation. Although neither IL-6 nor sIL-6R alone accelerated the differentiation, the combined use of the two markedly accelerated the differentiation of hVSMCs into osteoblast-like cells (Fig. 1B). Since hVSMCs do not express sIL-6R [17], these results indicate that differentiation of hVSMCs into osteoblast-like cells requires both IL-6 and sIL-6R. We also quantified the extent of calcification by using the OCPC method. TNF-α and IL-1β did not increase calcium deposition, whereas the presence of both IL-6 and sIL-6R increased calcium deposition at 100 ng/ml (Fig. 1C).

IL-6/sIL-6R accelerated RUNX2 expression and upregulated osteoblast differentiation-related genes.

Next, we investigated the effects of each inflammatory cytokine on the expression levels of genes associated with differentiation of osteoblasts and SMCs in hVSMCs by quantitative real-time polymerase chain reaction (RT-PCR). IL-6/sIL-6R, but not TNF-α and IL-1β, accelerated *RUNX2* messenger ribonucleic acid (mRNA) expression, the master gene for osteoblast differentiation, on day 3 of culture (Fig. 2A). We also examined the effects of other osteoblast-associated genes; IL-1β amplified the expression levels of *BMP-2* and *OPN*, while TNF-α increased *OPN* expression.

IL-6/sIL-6R enhanced the mRNA expression of *ALP* and *OPN,* which are osteoblast-specific genes, and reduced mRNA expression of *SM-MHC*, which is a SMCs-specific gene (Fig. 2A). *RUNX2* mRNA expression was accelerated by OIM only, but the effect was more pronounced following the addition of IL-6 and sIL-6R with a peak time at days 3 to 7 (Fig. 2B). Since the induction of gene expression of *RUNX2* reached a peak level at 3 days post-stimulation, we selected day 3 as the time interval for quantitative RT-PCR. Furthermore, IL-6/sIL-6R accelerated *RUNX2* mRNA expression in a dose-dependent manner (Fig. 2B).

Phosphorylation of STAT3 was important for IL-6/sIL-6R-induced differentiation of hVSMCs into osteoblast-like cells.

To determine the role of signal transducer and activator of transcription (STAT)s in IL-6-dependent differentiation of hVSMCs into osteoblast-like cells, we used western blotting (WB) by assessing the phosphorylation of STAT1 and STAT3, which are located downstream of the IL-6 signal. Stimulation for 10 min with IL-6/sIL-6R resulted in the phosphorylation of both STAT1 and STAT3 (Fig. 3A). Next, we used siRNAs to assess the separate effect of each transcription factor on the IL-6-dependent differentiation of VSMCs. The expression of STAT1 and STAT3 was effectively suppressed using two different siRNA sequences that targeted STAT1 (siSTAT1-#1 and siSTAT1-#2) or STAT3 (siSTAT3-#1 and siSTAT3-#2) (Fig. 3B, Supplementary Table). We then assessed the effects of STAT1 and STAT3 on calcification by ARS staining on culture day 21. Knockdown of STAT3, but not that of STAT1, reduced IL-6/sIL-6R induced differentiation into osteoblast-like cells (Fig. 3C). After 3-day culture under similar siRNA conditions, RT-PCR was performed to assess *RUNX2* and *SM-MHC* mRNA expression levels. Similar to the above results, knockdown of STAT3, but not that of STAT1, reduced IL-6/sIL-6R-induced *RUNX2* mRNA upregulation. Furthermore, knockdown of STAT3, but not that of STAT1, reduced IL-6/sIL-6R-induced *SM-MHC* mRNA downregulation (Fig. 3D). Also we quantified the effects of siSTAT3 for IL-6/sIL-6R-induced calcification by using the OCPC method. As shown in Supplementary Figure A, knockdown of STAT3, but not that of STAT1, reduced IL-6/sIL-6R induced calcium deposition (*Grey bars:* no stimulation, *solid bars:* IL-6/sIL-6R stimulation (100 ng/ml)). These results suggest that STAT3 phosphorylation plays a role in IL-6-dependent transformation of hVSMCs into osteoblast-like cells.

IL-6/sIL-6R-induced demethylation of H3K9me3 at the STAT-binding site in the RUNX2 promoter region.

To elucidate the relationship between changes in histone modification and STAT3-dependent differentiation of hVSMCs into osteoblast-like cells, we examined histone modification on the *RUNX2* promoter region after stimulation with or without IL-6/sIL-6R. Histone modifications were assessed in Region 1, which is located at 3000 base pairs upstream from the transcription start site (TSS) and contains no STAT-binding sites, and in Region 2, which is located at 1000 base pairs upstream from the TSS for *RUNX2* and contains STAT-binding sites, using chromatin immunoprecipitation (ChIP)-PCR (Fig. 4A, Supporting Information). In Region 2, the *RUNX2* locus was marked by bivalent histone modifications, such as permissive H3K4me3 and repressive H3K9me3. After 20 min of IL-6/sIL-6 stimulation, no changes were observed in either H3K9ac or H3K14ac, both of which are typical acetylated histones. With regard to methylated histones, although no changes were observed in H3K4me3, H3K27me3, or H3K36me3, the expression of only H3K9me3, an inhibitory marker, was strongly suppressed (Fig. 4B). In addition, IL-6/sIL-6R-dependent H3K9me3 suppression was abrogated by knockdown of STAT3 (Fig. 4C).

IL-6/sIL-6R-stimulation demethylated H3K9me3 through recruitment of JMJD2B.

Demethylation of H3K9me3 is assumed to result from recruitment of histone demethylases to the *RUNX2* promoter region. First, we confirmed the expression of JMJD2A, JMJD2B, JMJD2C, and JMJD2D, which are histone demethylases for H3K9me3, in hVSMCs by RT-PCR. However, the expression levels of these demethylases did not change regardless of stimulation of hVSMCs with or without IL-6/sIL-6R for 24 h (Fig. 5A, Supporting Information). We also confirmed protein expression in a relatively short time (20 min) in order to evaluate the translocation of proteins into the nucleus. We quantified the changes in JMJD2B protein level using nuclear extract, but there was no difference in the expression in WB at 20 min after stimulation with IL-6/sIL-6R

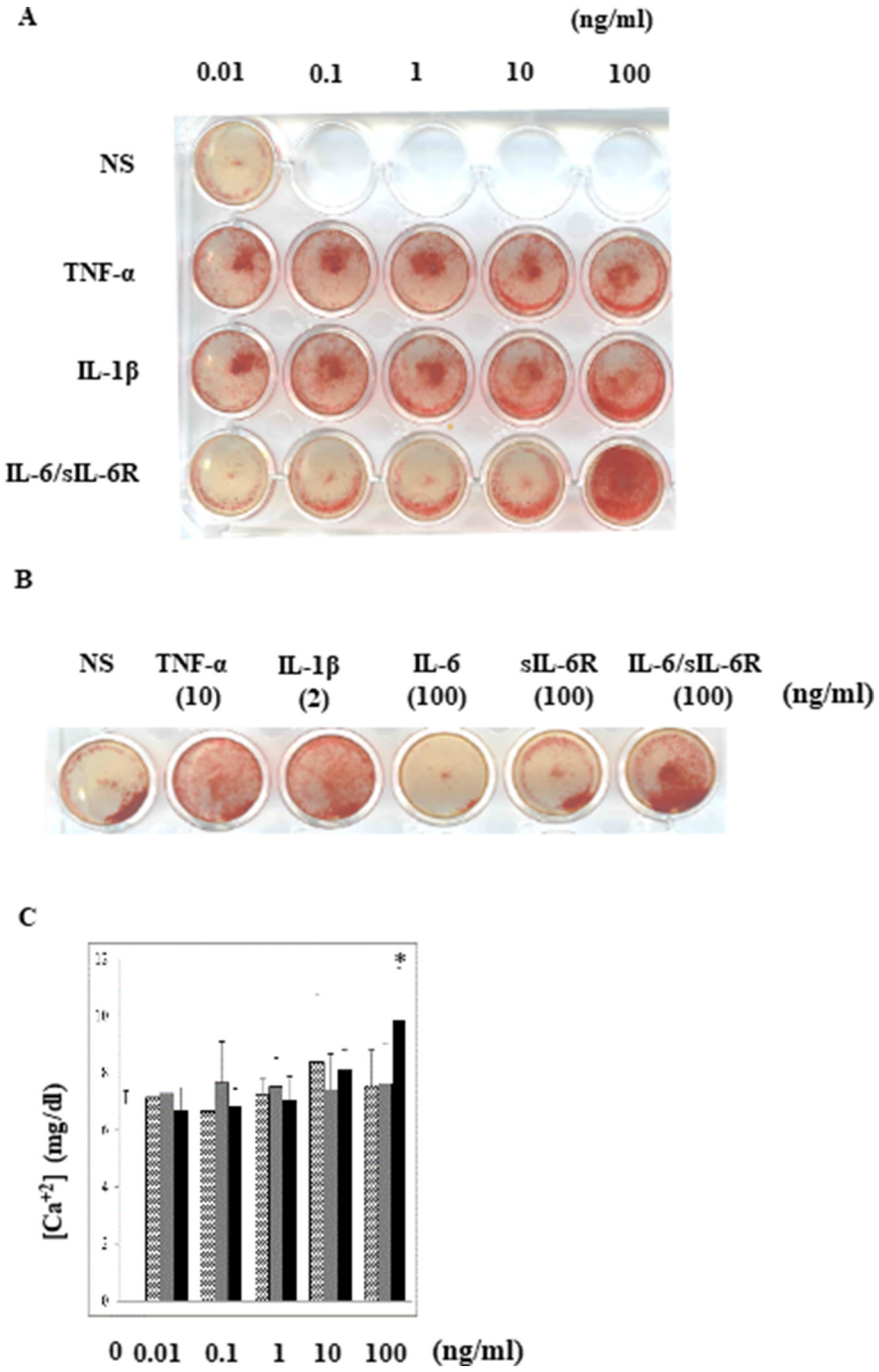

Fig. 1. IL-6/sIL-6R induces differentiation of hVSMCs into osteoblast-like cells.
(A) hVSMCs were cultured in OIM supplemented with TNF-α, IL-1β or IL-6/sIL-6R (0.01, 0.1, 1, 10 and 100 ng/ml). Cell calcification was evaluated by ARS staining on day 21. (B) hVSMCs were cultured in OIM supplemented with TNF-α (10 ng/ml), IL-1β (2 ng/ml), IL-6 (100 ng/ml), sIL-6R (100 ng/ml) or IL-6/sIL-6R (100 ng/ml). Cell calcification was evaluated by ARS staining on day 21. (C) Calcium contents in the HCl supernatant was determined colorimetrically by the OCPC method. hVSMCs were cultured in OIM supplemented with TNF-α, IL-1β or IL-6/sIL-6R at each concentration. *Open bar*: control (no stimulation), *hatched bars*: TNF-α, *grey bars*: IL-1β, *solid bars*: IL-6/sIL-6R stimulation. Data are mean ± SD of three independent experiments, each performed in triplicate. *$p < 0.05$ vs the control.

(data not shown). Although the expression of JMJD2B in the nuclei was upregulated relative to that of JMJD2A and JMJD2C, IL-6/sIL-6R stimulation did not change the expression level of any of these enzymes as determined by immunostaining (Fig. 5B). We also used ChIP-PCR to assess the effects of IL-6/sIL-6R stimulation on the recruitment of histone demethylases to the *RUNX2* promoter region. After 20-min IL-6/sIL-6R stimulation, JMJD2B expression was only increased in Region 2 (Fig. 5C). Also we analyzed the possible physical interaction between STAT3 and JMJD2 in VSMCs using immunoprecipitation (IP)-western blotting. As shown in Fig. 5D, STAT3 and JMJD2B are expressed in VSMCs in the absence or presence of IL-6/sIL-6R. We further found that IL-6/sIL-6R-stimulation enhanced association between JMJD2B and STAT3. Furthermore, induction of IL-6/sIL-6R-dependent *RUNX2* gene expression was inhibited in hVSMCs pretreated with JIB04, a JMJD2 inhibitor, at day 3, and this inhibitory effect was influenced by JIB04 dose-dependently (Fig. 5E). Also we assessed the effects of JIB04 at 1.0 μM for IL-6/sIL-6R-induced suppression of H3K9m3e at *RUNX2* promoter region. As shown in Supplementary Figure B, JIB04 at 1.0 μM canceled IL-6/sIL-6R-induced suppression of H3K9m3e at *RUNX2* promoter region. Next we assessed the effects of JMJD2B knockdown in hVSMCs in IL-6/sIL-6R induced osteoblastic trans-differentiation. As shown in Supplementary Figure C, we could knock down KDM4B (JMJD2B) by using Stealth siRNA KDM4B-#3 at 7.5 pmol (ThermoFisher, #3: HSS177107), but not by using Stealth siRNA KDM4B-#1, #2 (ThermoFisher, #1: HSS118058, #2: HSS177106). So we confirmed the effect of knock down of siRNA KDM4B-#3 for IL-6/sIL-6R induced calcification. As shown in Supplementary Figure D, knockdown of JMJD2B reduced IL-6/sIL-6R induced differentiation into osteoblast-like cells. These results suggest that demethylation of H3K9me3 occurs when phosphorylated (p)-STAT3, induced by IL-6/sIL-6R stimulation, is

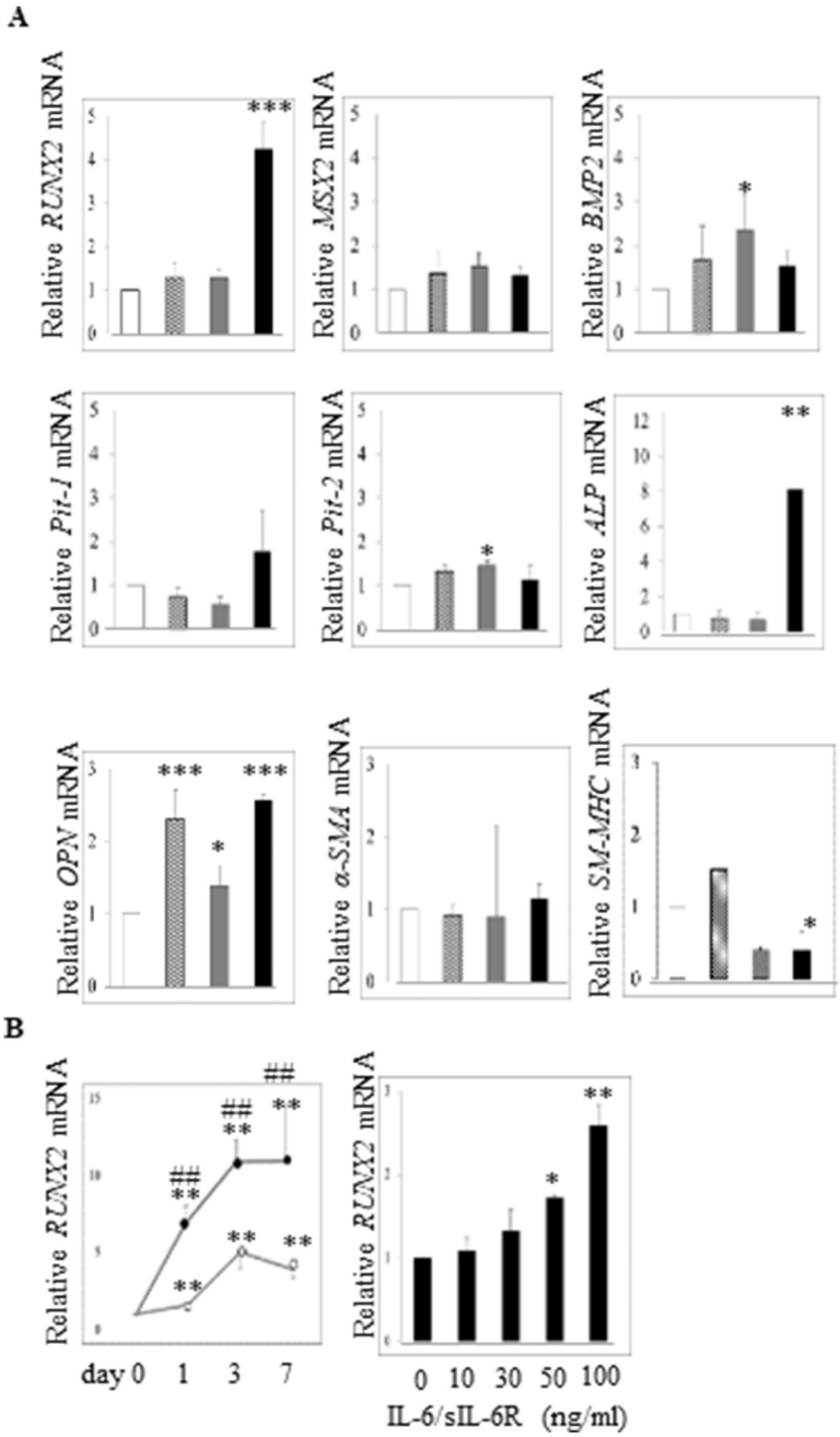

Fig. 2. IL-6/sIL-6R accelerates the expression of master gene for osteoblast differentiation and osteoblast-specific genes but reduces hVSMCs-specific gene.
(A) hVSMCs were cultured in OIM supplemented with TNF-α (10 ng/ml), IL-1β (2 ng/ml) or IL-6/sIL-6R (100 ng/ml). Total RNA was isolated at day 3 of culture. Gene expression levels were determined by RT-PCR. *p < 0.05, **p < 0.01, ***p < 0.001, vs no stimulation. (B) hVSMCs were cultured in OIM alone or OIM supplemented with IL-6/sIL-6R (100 ng/ml). Total RNA was isolated at days 1, 3 or 7 of culture (left side). hVSMCs were cultured in OIM alone or OIM supplemented with 10, 30, 50 and 100 ng/ml of IL-6/sIL-6R. Total RNA was isolated at day 3 of culture (right side). *Open bar:* control (no stimulation), *hatched bars:* TNF-α, *grey bars:* IL-1β, *solid bars:* IL-6/sIL-6R stimulation. Data are mean ± SD of three independent experiments, each performed in triplicate. **p < 0.01, vs day 0, ##p < 0.01, vs the control on the same day (left side). *p < 0.05, **p < 0.01, vs the control (no stimulation) (right side).

recruited together with JMJD2B to the STAT-binding sites in the *RUNX2* promoter region, and that such demethylation subsequently induces the transcription of *RUNX2* mRNA.

4. Discussion

Our study showed for the first time that the inflammatory cytokine IL-6 strongly induced differentiation of hVSMCs into osteoblast-like cells, and that such process was dependent on p-STAT3. The results also showed that the induction of *RUNX2* gene expression, a master transcription factor in osteoblast differentiation, required demethylation of H3K9me3 by recruiting JMJD2B, a histone demethylase, in addition to p-STAT3 in the promoter region.

IL-6/sIL-6R stimulation amplified the mRNA expression of *RUNX2*, as well as that of osteoblast differentiation markers such as *ALP* and *OPN*. On the other hand, although IL-6/sIL-6R stimulation suppressed

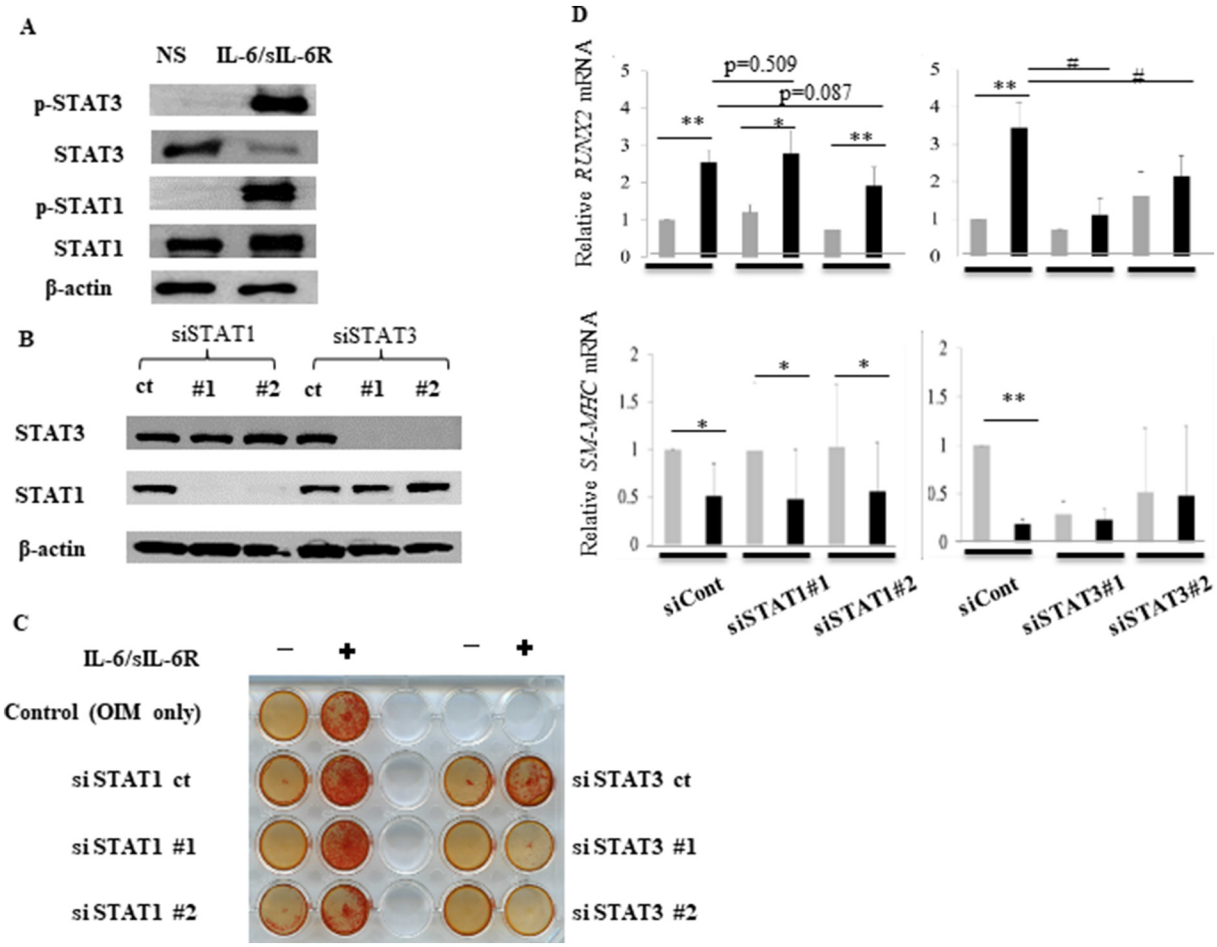

Fig. 3. IL-6/sIL-6R induces *RUNX2* expression and differentiation of hVSMCs into osteoblast-like cells is STAT3-dependent.
(A) hVSMCs were cultured in OIM alone or OIM supplemented with IL-6/sIL-6R (100 ng/ml) for 10 min. STAT1, STAT3, p-STAT1, p-STAT3 and β-actin were detected by western blotting. (B) hVSMCs were transfected with STAT1 (siSTAT1-#1 and siSTAT1-#2), STAT3 (siSTAT3-#1 and siSTAT3-#2) and control siRNA for 24 h. (C) Transfected hVSMCs were cultured in OIM alone or OIM supplemented with IL-6/sIL-6R (100 ng/ml) and ARS staining was performed on day 14. (D) Transfected hVSMCs were cultured in OIM with or without IL-6/sIL-6R (100 ng/ml). *Grey bars:* no stimulation, *solid bars:* IL-6/sIL-6R stimulation, Total RNA was isolated from transfected hVSMCs at day 3 of culture. Gene expression levels were determined by RT-PCR. Data are mean ± SD of three independent experiments, each performed in triplicate. *$p < 0.05$, **$p < 0.01$, vs no stimulation, #$p < 0.05$ vs siCont (OIM + IL-6/sIL-6R).

the expression of *SM-MHC*, a marker of VSMC differentiation, it did not affect that of *α-SMA*. These results suggest that IL-6/sIL-6R stimulation-induced transformation of hVSMCs into osteoblast-like cells is dependent on *RUNX2* expression but not on loss of the SMC lineage marker.

Although TNF-α and IL-1β slightly accelerated the differentiation of hVSMCs into osteoblast-like cells as demonstrated by ARS staining (Fig. 1A), our results showed that these two cytokines did not increase calcium deposition, as examined by the OCPC method (Fig. 1C). Also we observed ARS staining with an optical microscope and cells stimulated with IL-6/IL-6R-stimulation exhibited severe staining with numerous specific positive staining droplets, while cells stimulated with TNF-α or IL-1β did not stain intensely (Supplementary Figure E). Lin et al. warned against false positive results of ARS staining when fibroblasts change to myofibroblasts [18]. Accordingly, it is possible that the results of ARS staining for TNF-α and IL-1β were false-positive in the present study. We also measured the changes in ALP and SM-MHC protein levels by WB and estimated ALP and osteocalcin secretion by measuring their levels in cell culture supernatants. Unfortunately, we were unable to obtain meaningful results due to considerable variations among the samples.

In our study, induction of *RUNX2* gene expression by IL-1β and TNF-α could not be confirmed until at day 7 after stimulation. In this regard, Lee et al. reported that TNF-α increased *ALP* expression and *RUNX2* mRNA expression in human VSMCs [19], but the latter was evaluated in their experiments at day 14 after stimulation with TNF. It is unlikely that these results reflect direct induction by TNF.

Our results also confirmed that neither TNF-α nor IL-1β alone increase *IL-6R* gene expression in hVSMCs (data not shown). These results indicate that TNF-α and IL-1β cannot induce differentiation of hVSMCs into osteoblast-like cells in the absence of sIL-6R. Several studies reported that *BMP2* and *OPN* are NF-κB-target genes [20–22]. Since both IL-1β and TNF-α can activate NF-κB, these stimuli may increase the mRNA expression of both *BMP2* and *OPN*.

Several studies have indicated that p-STAT3 transport to the nucleus is important for IL-6-induced osteoblast-like differentiation [23–26]. In human mesenchymal stem cells (MSCs) derived from the bone marrow or adipose tissue, p-STAT3 is considered essential for oncostatin M (OSM)-induced osteoblast differentiation [27,28]. We reported previously that in human adipose-derived stromal cells, IL-6 activates tyrosine-protein kinase transmembrane receptor 2 (ROR2)/non-canonical wingless-type (WNT) 5A in a manner dependent on p-STAT3, and that such activation subsequently induces calcification [29]. Furthermore, Kakutani et al. reported in a study using hVSMCs that OSM enhanced osteoblast differentiation through activation of the Janus kinase 3 (JAK3)-STAT3 pathway [30]. The results of the present study are consistent with those of the above reports and highlight the importance of p-STAT3 in IL-6-dependent induction of calcification in hVSMCs.

Transformation of hVSMCs to osteoblast-like cells is dependent on

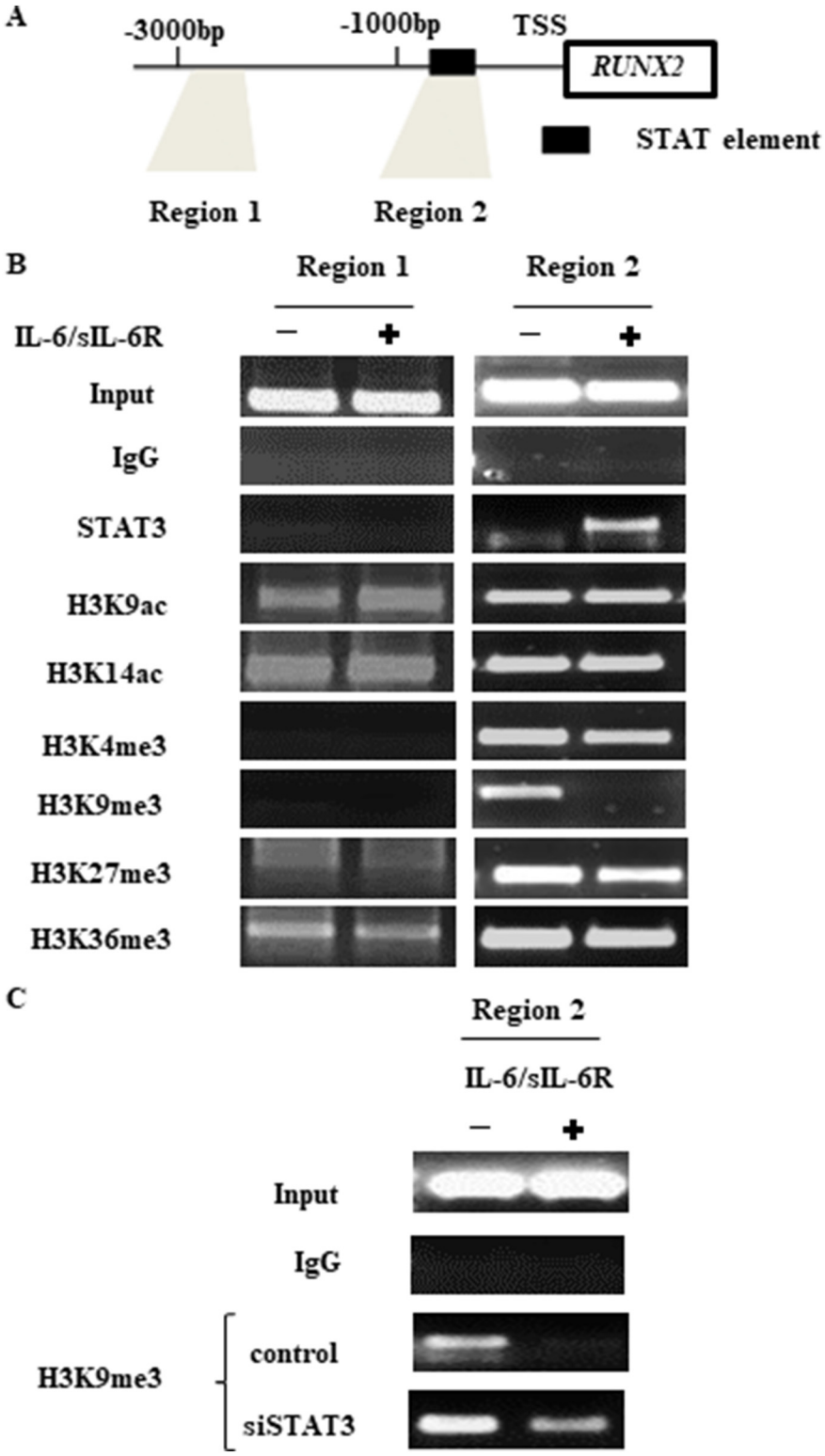

Fig. 4. IL-6/sIL-6R alters histone modification at *RUNX2* promoter region in hVSMCs.
(A) Histone modification of *RUNX2* at Regions 1 and 2 was assessed by ChIP-PCR. Region 1: non-STAT binding site and 3000 bp upstream from TSS, Region 2: STAT binding site and 1000 bp upstream from TSS. (B) hVSMCs were cultured in OIM alone or OIM supplemented with IL-6/sIL-6R (100 ng/ml) for 20 min. Histone modifications were assessed by ChIP-PCR. (C) hVSMCs were transfected with STAT3 or control siRNA for 24 h. H3K9me3 was assessed by ChIP-PCR at Region 2.

upregulation of *RUNX2*. Regulation of *RUNX2* transcription is considered to be associated with chromatin remodeling and acetylation of histone H3 and H4 [31]. Moreover, recent reports have also shown that JMJD2B and JMJD3 are essential for the transition of MSCs into the osteoblast lineage in human [32], suggesting major involvement in histone modifications. It is noteworthy that *RUNX2* gene expression was upregulated by bivalent histone modifications by transcriptional enhancer H3K4me3 and transcriptional repressor H3K9me3 in hVSMCs. This finding supports the plasticity of the process of hVSMCs differentiation. Although *RUNX2* gene expression is normally suppressed in

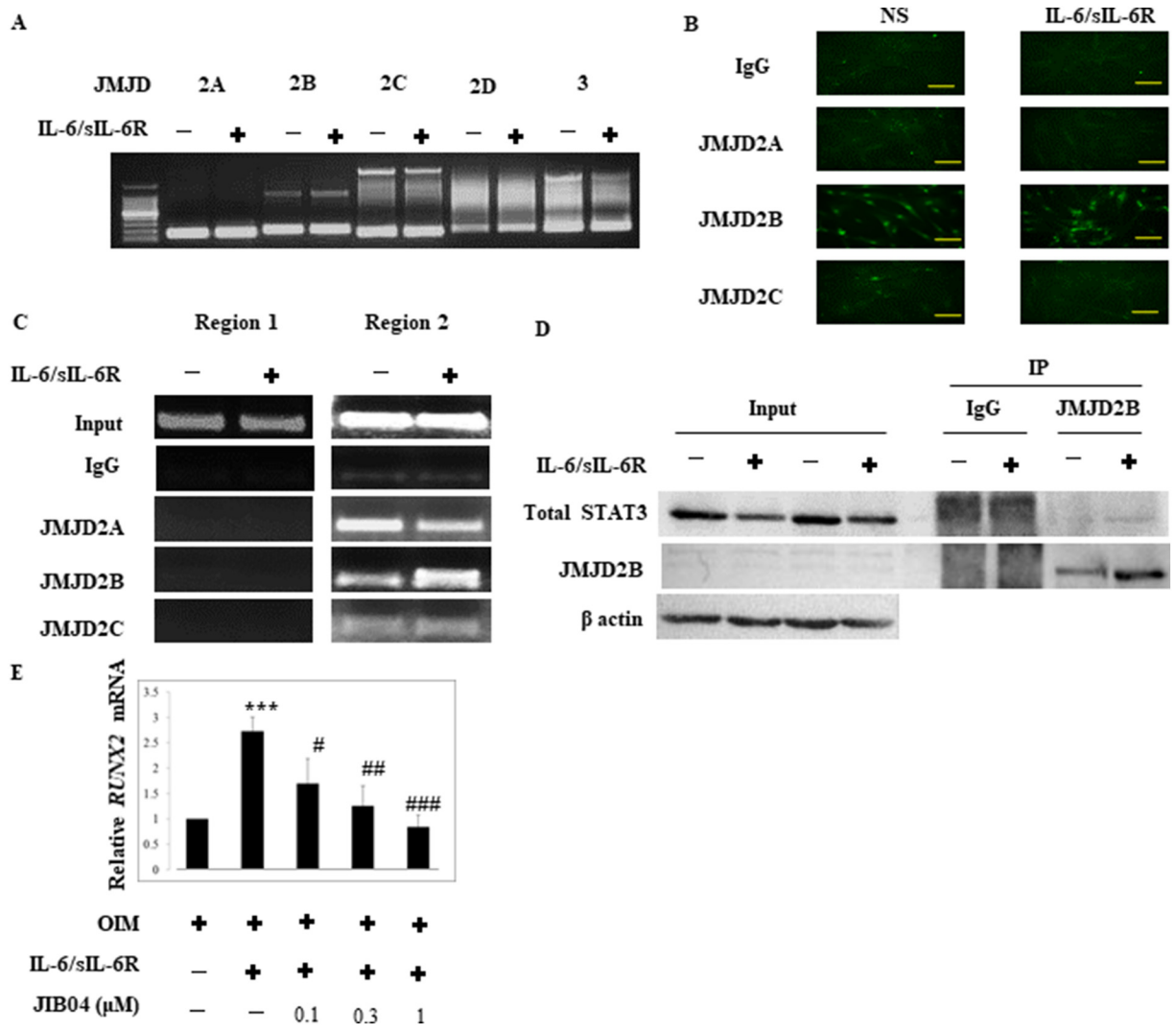

Fig. 5. JMJD2B is essential for IL-6/sIL-6R induced *RUNX2* expression in hVSMCs.
(A) hVSMCs were cultured in OIM alone or OIM supplemented with IL-6/sIL-6R (100 ng/ml) for 24 h. The expression level of JMJD2s in hVSMCs was assessed by RT-PCR. (B) hVSMCs were cultured in OIM alone or OIM supplemented with IL-6/sIL-6R (100 ng/ml) for 20 min. The expression of JMJD2s in hVSMCs was assessed by immunostaining. Yellow scale line: 100 μm. (C) hVSMCs were cultured in OIM alone or OIM supplemented with IL-6/sIL-6R (100 ng/ml) for 20 min. JMJD2 was assessed by the ChIP-PCR at Region 1 and Region 2. Region 1: non-STAT binding site and 3000 bp upstream from TSS, Region 2: STAT binding site and 1000 bp upstream from TSS. (D) hVSMCs were cultured in OIM alone or OIM supplemented with IL-6/sIL-6R (100 ng/ml) for 20 min. Association between STAT3 and JMJD2B were assessed by the IP-western blotting. (E) hVSMCs were cultured in OIM alone or OIM supplemented with IL-6/sIL-6R (100 ng/ml). hVSMCs was pretreated with JIB04, a JMJD2 inibitor, at 0.1, 0.3 and 1 μM. Total RNA was isolated at day 3 of culture. JMJD2B was detected by western blotting. Gene expression levels were determined by RT-PCR. ***p < 0.001, vs no stimulation, #p < 0.05 ##p < 0.01, ###p < 0.001, vs JIB04 free. (For interpretation of the references to color in this figure legend, the reader is referred to the web version of this article.)

hVSMCs, our results suggest enhanced *RUNX2* gene expression following IL-6/sIL-6R-induced p-STAT3 activation and recruitment of JMJD2B, which demethylates H3K9me3. With regard to the relation between histone methylation and calcification, it has been reported that osteoblast differentiation is enhanced by amplification of *RUNX2* through various pathways: *i)* by JMJD3 and the ubiquitously transcribed tetratricopeptide repeat X chromosome (UTX) [33,34], both of which are histone demethylases for H3K27me3, in MC3T3-E1 cells derived from murine calvaria, *ii)* by JMJD3 in dental MSCs [35], and by *iii)* Wolf-Hirschhorn syndrome candidate 1 (Whsc1), a histone demethylase for histone H3 lysine 36, in murine C3H 10 T1/2 cells and MC3T3-E1 cells [36].

Meanwhile, a histone modification pattern called the bivalent domain, in which two contradictory modifiers; transcriptional enhancer H3K4me3 and transcriptional repressor H3K9me3, coexist, was widely detected in the promoter regions of genes associated with murine development and differentiation and in embryonic stem cells (ESCs), and the bivalent domain balance is reported to be important in determining the fate of ESCs [37,38]. Matsumura et al. reported recently the presence of H3K4me3/H3K9me3 bivalent domain in the genes for *peroxisome proliferator-activated receptor g (Pparg)* and *CCAAT/enhancer binding protein α (Cebpa)*, which are master transcription factors involved in the differentiation of preadipocytes to adipocytes, and demonstrated that H3K9me3 inhibited differentiation of preadipocytes into adipocytes [39]. Since H3K9me3 also similarly inhibits the differentiation of hVSMCs into osteoblast-like cells, we suggest that H3K9me3 seems to be involved in the regulation of differentiation of both adipocytes and osteoblasts.

Since JMJD can activate ferrous iron or α-ketoglutarate (α-KG)-dependent demethylation of lysine, it is possible that members of the JMJD family can demethylate trimethyl-lysine, suggesting the presence of a JMJD2 cluster of enzymes that can demethylate H3K9me3, which

has been regarded as the most stable modification pattern [40–43]. The JMJD2 cluster consists of four genes; *JMJD2-A to -D*, which are expressed ubiquitously in almost all cells. Interestingly, however; the JMJD2B protein is particularly highly expressed in hVSMCs. It is likely that IL-6/sIL-6R stimulation leads to recruitment of JMJD2B to the STAT-targeting sites in the *RUNX2* promoter region, where it demethylates H3K9me3 and consequently enhances osteoblast differentiation.

Although the contribution of other pathways cannot be ruled out, our results point to the regulatory role of the IL-6/STAT3 pathway in the differentiation of hVSMCs to osteoblast-like cells as well as its pathogenic role in vascular calcification associated with chronic inflammation. New therapeutic approaches designed to tackle this pathway could be potentially useful in the prevention of vascular calcification associated with chronic inflammation, such as CKD.

Supplementary data to this article can be found online at https://doi.org/10.1016/j.bone.2019.04.006.

Competing interest statement

The authors have no competing interests to declare.

Funding sources

This research did not receive any specific grant from funding agencies in the public, commercial or not-for-profit sectors.

References

[1] P.D. Reaven, J. Sacks, Coronary artery and abdominal aortic calcification are associated with cardiovascular disease in type 2 diabetes, Diabetologia 48 (2005) 379–385.
[2] S. Okuno, E. Ishimura, K. Kitatani, Y. Fujino, K. Kohno, Y. Maeno, et al., Presence of abdominal aortic calcification is significantly associated with all-cause and cardiovascular mortality in maintenance hemodialysis patients, Am. J. Kidney Dis. 49 (2007) 417–425.
[3] R. Vattikuti, D.A. Towler, Osteogenic regulation of vascular calcification: an early perspective, Am. J. Physiol. Endocrinol. Metab. 286 (2004) E686–E696.
[4] J.S. Shao, J. Cai, D.A. Towler, Molecular mechanisms of vascular calcification: lessons learned from the aorta, Arterioscler. Thromb. Vasc. Biol. 26 (2006) 1423–1430.
[5] A. Shioi, H. Taniwaki, S. Jono, Y. Okuno, H. Koyama, K. Mori, et al., Mönckeberg's medial sclerosis and inorganic phosphate in uremia, Am. J. Kidney Dis. 38 (2001) S47–S49.
[6] Z.A. Massy, P. Stenvinkel, T.B. Drueke, The role of oxidative stress in chronic kidney disease, Semin. Dial. 22 (2009) 405–408.
[7] J. Buturović-Ponikvar, Renal replacement therapy in Slovenia: annual report 2001, Nephrol. Dial. Transplant. (2003) v53–v55 suppl 5.
[8] D.V. Barreto, F.C. Barreto, S. Liabeuf, M. Temmar, H.D. Lemke, C. Tribouilloy, et al., European Uremic Toxin Work Group (EUTox), Plasma interleukin-6 is independently associated with mortality in both hemodialysis and pre-dialysis patients with chronic kidney disease, Kidney Int. 77 (2010) 550–556.
[9] C. Caselli, M.A. De Graaf, V. Lorenzoni, D. Rovai, M. Marinelli, et al., HDL cholesterol, leptin and interleukin-6 predict high risk coronary anatomy assessed by CT angiography in patients with stable chest pain, Atherosclerosis 241 (2015) 55–61.
[10] R. Pecoits-Filho, P. Bárány, B. Lindholm, O. Heimbürger, P. Stenvinkel, Interleukin-6 is an independent predictor of mortality in patients starting dialysis treatment, Nephrol. Dial. Transplant. 17 (2002) 1684–1688.
[11] L. Hénaut, Z.A. Massy, New insights into the key role of interleukin 6 in vascular calcification of chronic kidney disease, Nephrol. Dial. Transplant. 33 (2018) 543–548.
[12] D. Zickler, C. Luecht, K. Willy, L. Chen, M. Grindt, et al., Tumour necrosis factor-alpha in uraemic serum promotes osteoblastic transition and calcification of vascular smooth muscle cells via extracellular signal-regulated kinases and activator protein 1/c-FOS-mediated induction of interleukin 6 expression, Nephrol. Dial. Transplant. 33 (2018) 574–585.
[13] M. Sun, Q. Chang, M. Xin, Q. Wang, H. Li, J. Qian, Endogenous bone morphogenetic protein 2 plays a role in vascular smooth muscle cell calcification induced by interleukin 6 in vitro, Int. J. Immunopathol. Pharmacol. 30 (2017) 227–237.
[14] S. Rajender, K. Avery, A. Agarwal, Epigenetics, spermatogenesis and male infertility, Mutat. Res. 727 (2011) 62–67.
[15] V.V. Lunyak, M.G. Rosenfeld, Epigenetic regulation of stem cell fate, Hum. Mol. Genet. 17 (2008) 28–36.
[16] C. Kasperk, J. Wergedal, D. Strong, J. Farley, K. Wangerin, H. Gropp, et al., Human bone cell phenotypes differ depending on their skeletal site of origin, J. Clin. Endocrinol. Metab. 80 (1995) 2511–2517.
[17] M. Klouche, S. Bhakdi, M. Hemmes, S. Rose-John, Novel path to activation of vascular smooth muscle cells: up-regulation of gp130 creates an autocrine activation loop by IL-6 and its soluble receptor, J. Immunol. 163 (1999) 4583–4589.
[18] N. Li, W. Cheng, T. Huang, J. Yuan, X. Wang, M. Song, Vascular adventitia calcification and its underlying mechanism, PLoS One 10 (2015) e0132506.
[19] H. Lee, K.M. Woo, H.M. Ryoo, J.H. Baek, Tumor necrosis factor-alpha increases alkaline phosphatase expression in vascular smooth muscle cells via MSX2 induction, Biochem. Biophys. Res. Commun. 391 (2010) 1087–1092.
[20] J.Q. Feng, L. Xing, J.H. Zhang, M. Zhao, D. Horn, J. Chan, et al., NF-kappaB specifically activates BMP-2 gene expression in growth plate chondrocytes in vivo and in a chondrocyte cell line in vitro, J. Biol. Chem. 278 (2003) 29130–29135.
[21] N. Fukui, Y. Ikeda, T. Ohnuki, A. Hikita, S. Tanaka, S. Yamane, et al., Pro-inflammatory cytokine tumor necrosis factor-alpha induces bone morphogenetic protein-2 in chondrocytes via mRNA stabilization and transcriptional up-regulation, J. Biol. Chem. 281 (2006) 27229–27241.
[22] R.S. Samant, D.W. Clark, R.A. Fillmore, M. Cicek, B.J. Metge, K.H. Chandramouli, et al., Breast cancer metastasis suppressor 1 (BRMS1) inhibits osteopontin transcription by abrogating NF-kappaB activation, Mol. Cancer 6 (2007) 6.
[23] S. Itoh, N. Udagawa, N. Takahashi, F. Yoshitake, H. Narita, S. Ebisu, et al., A critical role for interleukin-6 family-mediated Stat3 activation in osteoblast differentiation and bone formation, Bone 39 (2006) 505–512.
[24] T. Fukada, M. Hibi, Y. Yamanaka, M. Takahashi-Tezuka, Y. Fujitani, T. Yamaguchi, et al., Two signals are necessary for cell proliferation induced by a cytokine receptor gp130: involvement of STAT3 in anti-apoptosis, Immunity 5 (1996) 449–460.
[25] C. Gerhartz, B. Heesel, J. Sasse, U. Hemmann, C. Landgraf, J. Schneider-Mergener, et al., Differential activation of acute phase response factor/STAT3 and STAT1 via the cytoplasmic domain of the interleukin 6 signal transducer gp130. I. Definition of a novel phosphotyrosine motif mediating STAT1 activation, J. Biol. Chem. 271 (1996) 12991–12998.
[26] Y. Yamanaka, K. Nakajima, T. Fukada, M. Hibi, T. Hirano, Differentiation and growth arrest signals are generated through the cytoplasmic region of gp130 that is essential for Stat3 activation, EMBO J. 15 (1996) 1557–1565.
[27] H.Y. Song, E.S. Jeon, J.I. Kim, J.S. Jung, J.H. Kim, Oncostatin M promotes osteogenesis and suppresses adipogenic differentiation of human adipose tissue-derived mesenchymal stem cells, J. Cell. Biochem. 101 (2007) 1238–1251.
[28] P. Guihard, Y. Danger, B. Brounais, E. David, R. Brion, J. Delecrin, et al., Induction of osteogenesis in mesenchymal stem cells by activated monocytes/macrophages depends on oncostatin M signaling, Stem Cells 30 (2012) 762–772.
[29] S. Fukuyo, K. Yamaoka, K. Sonomoto, K. Oshita, Y. Okada, K. Saito, et al., IL-6-accelerated calcification by induction of ROR2 in human adipose tissue-derived mesenchymal stem cells is STAT3 dependent, Rheumatology 53 (2014) 1282–1290.
[30] Y. Kakutani, A. Shioi, T. Shoji, H. Okazaki, H. Koyama, M. Emoto, et al., Oncostatin M promotes osteoblastic differentiation of human vascular smooth muscle cells through JAK3-STAT3 pathway, J. Cell. Biochem. 116 (2015) 1325–1333.
[31] F. Cruzat, B. Henriquez, A. Villagra, M. Hepp, J.B. Lian, A.J. van Wijnen, et al., SWI/SNF-independent nuclease hypersensitivity and an increased level of histone acetylation at the P1 promoter accompany active transcription of the bone master gene Runx2, Biochemistry 48 (2009) 7287–7295.
[32] L. Ye, Z. Fan, B. Yu, J. Chang, K. Al Hezaimi, X. Zhou, et al., Histone demethylases KDM4B and KDM6B promotes osteogenic differentiation of human MSCs, Cell Stem Cell 11 (2012) 50–61.
[33] D. Yang, H. Okamura, Y. Nakashima, T. Haneji, Histone demethylase Jmjd3 regulates osteoblast differentiation via transcription factors Runx2 and osterix, J. Biol. Chem. 288 (2013) 33530–33541.
[34] D. Yang, H. Okamura, J. Teramachi, T. Haneji, Histone demethylase Utx regulates differentiation and mineralization in osteoblasts, J. Biol. Chem. 11 (2015) 2628–2636.
[35] J. Xu, B. Yu, C. Hong, CY. Wang, KDM6B epigenetically regulates odontogenic differentiation of dental mesenchymal stem cells, Int. J. Oral Sci. 5 (2013) 200–205.
[36] Y.F. Lee, K. Nimura, W.N. Lo, K. Saga, Y. Kaneda, Histone H3 lysine 36 methyltransferase Whsc1 promotes the association of Runx2 and p300 in the activation of bone-related genes, PLoS One 9 (2014) e106661.
[37] B.E. Bernstein, T.S. Mikkelsen, X. Xie, M. Kamal, D.J. Huebert, J. Cuff, et al., A bivalent chromatin structure marks key developmental genes in embryonic stem cells, Cell 125 (2006) 315–326.
[38] N.L. Vastenhouw, A.F. Schier, Bivalent histone modifications in early embryogenesis, Curr. Opin. Cell Biol. 24 (2012) 374–386.
[39] Y. Matsumura, R. Nakaki, T. Inagaki, A. Yoshida, Y. Kano, H. Kimura, et al., H3K4/H3K9me3 bivalent chromatin domains targeted by lineage-specific DNA methylation pauses adipocyte differentiation, Mol. Cell 60 (2015) 584–596.
[40] Y. Tsukada, J. Fang, H. Erdjument-Bromage, M.E. Warren, C.H. Borchers, P. Tempst, et al., Histone demethylation by a family of JmjC domain-containing proteins, Nature 439 (2006) 811–816.
[41] P.A. Cloos, J. Christensen, K. Agger, A. Maiolica, J. Rappsilber, T. Antal, et al., The putative oncogene GASC1 demethylates tri- and dimethylated lysine 9 on histone H3, Nature 442 (2006) 307–311.
[42] B.D. Fodor, S. Kubicek, M. Yonezawa, R.J. O'Sullivan, R. Sengupta, L. Perez-Burgos, et al., Jmjd2b antagonizes H3K9 trimethylation at pericentric heterochromatin in mammalian cells, Genes Dev. 20 (2006) 1557–1562.
[43] J.R. Whetstine, A. Nottke, F. Lan, M. Huarte, S. Smolikov, Z. Chen, et al., Reversal of histone lysine trimethylation by the JMJD2 family of histone demethylases, Cell 125 (2006) 467–481.